

1

2 A highly contiguous genome assembly for the Yellow Warbler

3 (*Setophaga petechia*)

4

5 Whitney L. E. Tsai^{1,2}, Merly Escalona³, Kimball L. Garrett⁴, Ryan S. Terrill², Ruta Sahasrabudhe⁵,
6 Oanh Nguyen⁵, Eric Beraut⁶, William Seligmann⁶, Colin W. Fairbairn⁶, Ryan J. Harrigan¹, John
7 E. McCormack², Michael E. Alfaro¹, Thomas B. Smith¹, Rachael A. Bay⁷

8

9 ¹Department of Ecology and Evolutionary Biology, University of California, Los Angeles, CA
10 90095

11 ²Moore Laboratory of Zoology, Occidental College, Los Angeles, CA 90041

12 ³Department of Biomolecular Engineering, University of California, Santa Cruz, CA 95064

13 ⁴Natural History Museum of Los Angeles County, Los Angeles, CA 90007

14 ⁵DNA Technologies and Expression Analysis Core Laboratory, Genome Center, University of
15 California, Davis, CA 95616

16 ⁶Department of Ecology and Evolutionary Biology, University of California, Santa Cruz, CA
17 95064

18 ⁷Department of Evolution and Ecology, University of California, Davis, CA 95616

19 **Corresponding author email:** whitney.le.tsai@gmail.com

20 **Running title:** Yellow Warbler reference genome assembly

21

22

23 **Abstract**

24 The Yellow Warbler (*Setophaga petechia*) is a small songbird in the New World Warbler family
25 (Parulidae) that exhibits phenotypic and ecological differences across a widespread distribution
26 and is important to California's riparian habitat conservation. Here, we present a high-quality *de*
27 *novo* genome assembly of a vouchered female Yellow Warbler from southern California. Using
28 HiFi long-read and Omni-C proximity sequencing technologies, we generated a 1.22 Gb assembly
29 including 687 scaffolds with a contig N50 of 6.80 Mb, scaffold N50 of 21.18 Mb, and a BUSCO
30 completeness score of 96.0%. This highly contiguous genome assembly provides an essential
31 resource for understanding the history of gene flow, divergence, and local adaptation and can
32 inform conservation management of this charismatic bird species.

33

34 **Keywords**

35 California Conservation Genomics Project, CCGP, Parulidae

36

37

38

39 **Introduction**

40 The Yellow Warbler (*Setophaga petechia*) is a widespread songbird species distributed from
41 Alaska to northern South America (Figure 1). The species complex comprises up to 43 subspecies
42 in four distinct subspecies groups that display notable diversity in phenotype and ecology across
43 their range (Browning, 1994; Klein & Brown, 1994; Salgado-Ortiz et al., 2008; Wilson &
44 Holberton, 2004). This phenotypic diversity and the presence of both migratory and resident
45 populations have encouraged investigation into the history of adaptation, divergence, and gene
46 flow in this species (Chavarria-Pizarro et al., 2019; Chaves et al., 2012; Gibbs et al., 2000;
47 Machkour-M'Rabet et al., 2023; Milot et al., 2000). Additionally, as a widespread migratory bird
48 species, the Yellow Warbler inhabits variable environmental conditions across its range, allowing
49 for the investigation into the influence of climate on geographic variation and genomic capacity to
50 adapt to climate change (Bay et al., 2018; Chen et al., 2022; DeSaix et al., 2022).

51 In California, Yellow Warblers are listed as a Species of Special Concern (Shuford et al.,
52 2008) and have experienced notable declines over the last 50 years (Sauer et al., 2014). Previous
53 genomic work indicates that the inability to adapt to climate change may play a role in population
54 declines in California (Bay et al., 2018). California wetlands and riparian corridors are crucial
55 stopover and breeding habitats for Yellow Warblers and other species of migratory birds. In the
56 last century, 90-95% of historic wetland and riparian habitats have been lost, and those that remain
57 are threatened by development and climate change (Dahl, 1990; Krueper, 1996; Poff et al., 2012).
58 As indicators of healthy riparian habitat, understanding how California Yellow Warbler
59 populations adapt to dramatic changes in their environment will inform conservation action and
60 help mitigate habitat loss in other vulnerable and threatened riparian species, like the California
61 Red-legged Frog (*Rana draytonii*), the Riparian Brush Rabbit (*Sylvilagus bachmani riparius*), and

62 the Valley Elderberry Longhorn Beetle (*Desmocerus californicus dimorphus*) (Collinge et al.,
63 2001; Davidson et al., 2001; Heath & Ballard, 2003; Phillips et al., 2005).

64 The evolutionary and conservation genomics studies needed to address these questions
65 increasingly rely on low-coverage, whole genome sequencing (WGS), which requires a high-
66 quality reference genome for alignment. Reference genome assemblies provide a map of the
67 structural features and organization of the genome and the choice of reference genome assembly
68 for WGS studies can impact evolutionary inferences like demographic history and genetic
69 diversity (Gopalakrishnan et al., 2017). Currently, there are four genome assemblies generated
70 with short-read sequencing technology for the genus *Setophaga*. There is one Yellow-rumped
71 Warbler (*S. coronata*) chromosome-level assembly (Toews et al., 2016), two Kirtland's Warbler
72 (*S. kirtlandii*) scaffold-level assemblies (Feng et al., 2020), and the existing draft genome assembly
73 for Yellow Warbler has a length of 1.26 Gb, a total of 18,414 scaffolds, and a scaffold N50 491.7
74 kb (Bay et al., 2018). The use of an interspecific reference genome assembly can lead to many
75 errors and biases, including lower mapping ability (especially in regions with higher evolutionary
76 rates) and inaccurate gene order (Prasad et al., 2022). The high number and relatively short scaffold
77 length of the existing Yellow Warbler genome assembly could hinder the identification of
78 structural variants often maintained between and within species and are important in adaptive
79 evolution, speciation, and generating morphological diversity (Lamichhaney et al., 2016; Mérot et
80 al., 2020; Wellenreuther & Bernatchez, 2018). Additionally, reference genome assemblies
81 generated solely from short-read sequencing technology fail to resolve lengths and placement of
82 repeat regions, such as transposable elements or telomeres, leading to gaps in avian genome
83 assemblies (Peona et al., 2021). This highlights the need for a high-quality, species-specific
84 reference genome for WGS studies.

85 Here, we present a new genome assembly for the Yellow Warbler generated as part of the
86 California Conservation Genomics Project (CCGP) consortium (Shaffer et al., 2022). We used
87 high-molecular-weight (HMW) genomic DNA (gDNA) extracted from a vouchered, female bird
88 collected in California and leveraged Pacific Biosciences (PacBio) HiFi long-read and Dovetail
89 Genomics Omni-C proximity sequencing technologies. This produced a high-quality genome
90 assembly that will allow us to better understand evolutionary processes like phenotypic variation
91 and migration and conduct conservation genomics studies to inform conservation initiatives.

92

93 **Methods**

94 *Biological Materials*

95 We sampled muscle, liver, and other tissues from a female Yellow Warbler collected using mist
96 nets near Stephen Sorensen Park (34.60549°N, 117.8306°W) in Los Angeles County, California
97 on September 25, 2020. This migrant Yellow Warbler can presumably be assigned to *S. p.*
98 *brewsteri* based on collection date and locality (Browning, 1994) and was collected with approval
99 from the following entities: California Department of Fish and Wildlife Scientific Collecting
100 Permit (#SC-000939), US Fish and Wildlife Services Scientific Collecting Permit (MB708062-0),
101 and US Geological Survey Banding Permit (22804-B). Tissue samples were retrieved and flash-
102 frozen in liquid nitrogen, and the first muscle tissues were frozen within two minutes of specimen
103 collection. A voucher specimen and tissue are deposited at the Natural History Museum of Los
104 Angeles (LACM Bird #122168, KLG4550, LAF9440). Additional tissues for this individual are
105 housed in the CCGP tissue repository at the University of California, Los Angeles under
106 identification YEWA_CCGP3.

107

108 *Nucleic acid extraction, library preparation, and sequencing*

109 We extracted HMW gDNA from 30mg of flash-frozen heart tissue. We homogenized the tissue

110 by grinding it in a mortar and pestle in liquid nitrogen. We lysed the homogenized tissue at room

111 temperature overnight with 2 ml of lysis buffer containing 100mM NaCl, 10 mM Tris-HCl pH 8.0,

112 25 mM EDTA, 0.5% (w/v) SDS, and 100µg/ml Proteinase K. We treated the lysate with 20µg/ml

113 RNAse at 37°C for 30 minutes. We cleaned the lysate with equal volumes of phenol/chloroform

114 using phase lock gels (Quantabio, MA; Cat # 2302830). We precipitated the DNA from the cleaned

115 lysate by adding 0.4X volume of 5M ammonium acetate and 3X volume of ice-cold ethanol. We

116 washed the pellet twice with 70% ethanol and resuspended it in elution buffer (10mM Tris, pH

117 8.0). We measured DNA purity using absorbance ratios (260/280 = 1.87 and 260/230 = 2.29) using

118 a NanoDrop ND-1000 spectrophotometer. We quantified DNA yield (30µg) using a Qubit 2.0

119 Fluorometer (Thermo Fisher Scientific, MA). We verified HMW gDNA integrity on a Femto pulse

120 system (Agilent Technologies, CA), where 80% of the DNA was found in fragments above 120

121 Kb.

122 According to the manufacturer's instructions, we constructed the HiFi Single Molecule,

123 Real-Time (SMRT) library using SMRTbell Express Template Prep Kit v2.0 (PacBio, CA; Cat.

124 #100-938-900). We sheared HMW gDNA to a target DNA size distribution between 15 – 20 kb

125 and concentrated it using 0.45X of AMPure PB beads (PacBio; Cat. #100-265-900). We performed

126 the enzymatic incubations as follows: removal of single-strand overhangs at 37°C for 15 minutes,

127 DNA damage repair at 37°C for 30 minutes, end repair at 20°C for 10 minutes, A-tailing at 65°C

128 for 30 minutes, ligation of overhang adapter v3 at 20°C for 60 minutes, ligase inactivation at 65°C

129 for 10 minutes, and nuclease treatment at 37°C for 1 hour. We purified and concentrated the library

130 with 0.45X Ampure PB beads for size selection to collect fragments greater than 7-9 kb using the

131 BluePippin/PippinHT system (Sage Science, MA; Cat #BLF7510/HPE7510). The HiFi library
132 averaged 15 – 20 kb. It was sequenced at UC Davis DNA Technologies Core (Davis, CA) using
133 two 8M SMRT cells, Sequel II sequencing chemistry 2.0, and 30-hour movies each on a PacBio
134 Sequel II sequencer.

135 We used the Omni-C™ Kit (Dovetail Genomics, CA) for Omni-C proximity sequencing
136 according to the manufacturer’s protocol with slight modifications. First, we ground muscle tissue
137 (Sample YEWA_CCGP3; LACM Bird #122168, KLG4550, LAF9440) with a mortar and pestle
138 while cooled with liquid nitrogen. Subsequently, chromatin was fixed in place in the nucleus. We
139 passed the suspended chromatin solution through 100 µm and 40 µm cell strainers to remove large
140 debris. We digested fixed chromatin under various conditions of DNase I until a suitable fragment
141 length distribution of DNA molecules was obtained. We repaired chromatin ends, ligated a
142 biotinylated bridge adapter, and performed proximity ligation of adapter-containing ends. After
143 proximity ligation, crosslinks were reversed, and the DNA was purified from proteins. We treated
144 purified DNA to remove biotin that was not internal to ligated fragments. We generated a next-
145 generation sequencing library using an NEB Ultra II DNA Library Prep kit (New England Biolabs,
146 MA) with an Illumina-compatible y-adapter. Then, we captured biotin-containing fragments using
147 streptavidin beads. We split the post-capture product into two replicates before PCR enrichment
148 to preserve library complexity, with each replicate receiving unique dual indices. The library was
149 sequenced at the Vincent J. Coates Genomics Sequencing Lab (Berkeley, CA) on an Illumina
150 NovaSeq platform 6000 (Illumina, CA) to generate approximately 100 million 2 x 150 bp read
151 pairs per GB genome size.

152

153 *Nuclear genome assembly*

154 We assembled the Yellow Warbler genome following the CCGP assembly pipeline Version 4.0, as
155 outlined in Table 1, which lists the tools and non-default parameters used in the assembly. The
156 pipeline uses PacBio HiFi reads and Omni-C data to produce high-quality and highly contiguous
157 genome assemblies, minimizing manual curation. We removed remnant adapter sequences from
158 the PacBio HiFi dataset using HiFiAdapterFilt (Sim et al., 2022). Then, we obtained the initial
159 phased diploid assembly using HiFiasm (Cheng et al., 2022) with the filtered PacBio HiFi reads
160 and the Omni-C dataset. We aligned the Omni-C data to both assemblies following the Arima
161 Genomics Mapping Pipeline (https://github.com/ArimaGenomics/mapping_pipeline) and then
162 scaffolded both assemblies with SALSA (Ghurye et al., 2017, 2019).

163 We generated Omni-C contact maps for both assemblies by aligning the Omni-C data with
164 BWA-MEM (Li, 2013), identified ligation junctions, and generated Omni-C pairs using pairtools
165 (Goloborodko et al., 2018). We generated a multi-resolution Omni-C matrix with a cooler
166 (Abdennur & Mirny, 2020) and balanced it with hicExplorer (Ramírez et al., 2018). We used
167 HiGlass [Version 2.1.11] (Kerpedjiev et al., 2018) and the PretextSuite (<https://github.com/wtsi-hpag/PretextView>; <https://github.com/wtsi-hpag/PretextMap>; <https://github.com/wtsi-hpag/PretextSnapshot>) to visualize the contact maps and then we checked the contact maps for
168 major mis-assemblies. In detail, if we identified a strong off-diagonal signal and a lack of signal
169 in the consecutive genomic region in the proximity of a join made by the scaffolder, we dissolved
170 it by breaking the scaffolds at the coordinates of the join. After this process, no further manual
171 joins were made. Some remaining gaps (joins generated by the scaffolder) were closed using the
172 PacBio HiFi reads and YAGCloser (<https://github.com/merlyescalona/yagcloser>). Finally, we
173 checked for contamination using the BlobToolKit Framework (Challis et al., 2020). Given the

176 fragmentation of the assemblies, these were tagged as primary or alternate based on overall
177 metrics.

178

179 *Genome assembly assessment*

180 We generated k-mer counts from the PacBio HiFi reads using meryl
181 (<https://github.com/marbl/meryl>). The k-mer database was then used in GenomeScope2.0
182 (Ranallo-Benavidez et al., 2020) to estimate genome features, including genome size,
183 heterozygosity, and repeat content. To obtain general contiguity metrics, we ran QUAST
184 (Gurevich et al., 2013). To evaluate genome quality and functional completeness, we used BUSCO
185 (Manni et al., 2021) with the Aves ortholog database (aves_odb10) containing 8,338 genes. Base
186 level accuracy (QV) and k-mer completeness were assessed using the previously generated meryl
187 database and merqury (Rhie et al., 2020). We further estimated genome assembly accuracy via
188 BUSCO gene set frameshift analysis using the pipeline described in (Korlach et al., 2017).
189 Measurements of the size of the phased blocks are based on the size of the contigs generated by
190 HiFiasm on HiC mode. We follow the quality metric nomenclature established by (Rhie et al.,
191 2021), with the genome quality code x.y. P.Q.C, where x = log10[contig NG50]; y = log10[scaffold
192 NG50]; P = log10 [phased block NG50]; Q = Phred base accuracy QV (quality value); C = %
193 genome represented by the first 'n' scaffolds, following a known karyotype of 2n =80 for *S.*
194 *petechia* (Bird Chromosome Database, Chromosome number data V3.0/2022 - (Degrandi et al.,
195 2020; Hobart, 1991)). Quality metrics for the notation were calculated on the primary assembly
196 (bSetPet1.0.p).

197

198 *Mitochondrial genome assembly*

199 We assembled the mitochondrial genome of *S. petechia* from the PacBio HiFi reads using the
200 reference-guided pipeline MitoHiFi (Allio et al., 2020; Uliano-Silva et al., 2021). We used the
201 mitochondrial sequence of *Setophaga kirtlandii* (NCBI:NC_051027.1) as the starting reference
202 sequence. After completion of the nuclear genome, we searched for matches of the resulting
203 mitochondrial assembly sequence in the nuclear genome assembly using BLAST+ (Camacho et
204 al., 2009) and filtered out contigs and scaffolds from the nuclear genome with a percentage of
205 sequence identity >99% and size smaller than the mitochondrial assembly sequence.

206

207 **Results**

208 *Sequencing Data*

209 The Omni-C and PacBio HiFi sequencing libraries generated 85.3 million read pairs and 2.7
210 million reads, respectively. The latter yielded 40.87-fold coverage (N50 read length 17,523 bp;
211 minimum read length 41 bp; mean read length 17,110 bp; maximum read length of 54,497 bp).
212 Based on PacBio HiFi reads, we estimated a genome assembly size of 1.14 Gb, 0.245% sequencing
213 error rate and 1.16% nucleotide heterozygosity rate using Genomescope2.0. The k-mer spectrum
214 based on PacBio HiFi reads shows (Figure 2A) a bimodal distribution with two major peaks at 19-
215 and 39-fold coverage, where peaks correspond to homozygous and heterozygous states of a diploid
216 species.

217

218 *Nuclear genome assembly*

219 The final assembly consists of two haplotypes tagged as primary and alternate (bSetPet1.0.p and
220 bSetPet1.0.a). Both genome assembly sizes are similar but not equal to the estimated value from
221 Genomescope2.0 (Figure 2A). The primary assembly (bSetPet1.0.p) consists of 687 scaffolds

222 spanning 1.22 Gb with contig N50 of 6.8 Mb, scaffold N50 of 21.18 Mb, longest contig of 53.52
223 Mb, and largest scaffold of 66.28 Mb. The alternate assembly (bSetPet1.0.a) consists of 530
224 scaffolds, spanning 1.24 Gb with contig N50 of 8.3Mb, scaffold N50 of 21.18 Mb, largest contig
225 40.02 Mb and largest scaffold of 74.56 Mb. The Omni-C contact maps suggest highly contiguous
226 primary and alternate assemblies (Figure 2C and Supplementary Figure S1B). The primary
227 assembly has a BUSCO completeness score of 96.0% using the Aves gene set, a per-base quality
228 (QV) of 62.34, a k-mer completeness of 84.95, and a frameshift indel QV of 41.54. In comparison,
229 the alternate assembly has a BUSCO completeness score of 93.5% using the same gene set, a per-
230 base quality (QV) of 62.79, a k-mer completeness of 81.57, and a frameshift indel QV of 40.43.

231 During manual curation, we identified 13 misassemblies requiring breaking nine joins on
232 the primary assembly and four on the alternate assembly. We were able to close a total of five
233 gaps, three on the primary and two on the alternate assembly. We removed two contigs, one per
234 assembly, corresponding to mitochondrial contaminants. Detailed assembly statistics are reported
235 in Table 2, and a graphical representation of the primary assembly in Figure 2B (see
236 Supplementary Figure S1A for the alternate assembly). We have deposited both assemblies on
237 NCBI (See Table 2 and Data Availability for details).

238

239 *Mitochondrial genome assembly*

240 We assembled a mitochondrial genome with MitoHiFi. The final mitochondrial assembly has a
241 size of 16,809 bp. The base composition of the final assembly version is A=30.19%, C=31.77%,
242 G=14.19%, T=23.85%, and consists of 22 unique transfer RNAs and 13 protein-coding genes.

243

244 **Discussion**

245 Here, we present a highly contiguous genome assembly for the Yellow Warbler with two pseudo
246 haplotypes. Our genome assemblies meet thresholds for proposed quality standards for vertebrate
247 and avian genomes (Jarvis, 2016; Kapusta & Suh, 2017; Rhie et al., 2021). Compared to the
248 existing *Setophaga* genomes, the primary Yellow Warbler genome assembly presented here has
249 the highest BUSCO completeness (96.0% of Aves orthologs present) and the highest contig N50
250 (6.8 Mb). Although the Yellow-rumped and Kirtland's Warbler genome assemblies have higher
251 scaffold N50 values, our Yellow Warbler genome assembly has the fewest gaps greater than 5 N's
252 (284 compared to 49-67K in other *Setophaga* genome assemblies), which highlights the
253 improvement gained when using long-read sequencing technology in combination with short reads
254 for more contiguous and complete genomes.

255 The reference genome presented here provides an essential resource for evolutionary
256 research and conservation efforts in California and beyond. Future range-wide genomic analyses
257 will facilitate investigations into the history of gene flow and divergence between the various
258 subspecies groups in this complex (Browning, 1994; Chaves et al., 2012; Machkour-M'Rabet et
259 al., 2023). This system-wide genomic context lends itself to investigations into the genetic basis
260 underlying both phenotypic diversity and the evolution of migration (Aguillon et al., 2021;
261 Caballero-López et al., 2022; Delmore et al., 2020; Franchini et al., 2017; Toews et al., 2016).
262 Future landscape genomic analyses investigating environmental associations with genomic
263 variation could identify loci important for local adaptation in this widespread species (Bay et al.,
264 2018; Chen et al., 2022; Forester et al., 2018). Using this framework with future climate models
265 will allow for predictions of how Yellow Warblers may adapt to future climate change and identify
266 both populations that are likely to persist in and vulnerable to future climate change regimes, which
267 will guide local conservation implementation (Fitzpatrick & Keller, 2015; Shaffer et al., 2022).

268 This will be especially important for California populations experiencing population declines and
269 dwindling breeding habitat, which could benefit from direct conservation and management efforts
270 (Heath & Ballard, 2003; Shuford et al., 2008). Overall, the Yellow Warbler genome presented here
271 provides a key resource for investigating phenotypic and ecological evolution and conservation in
272 this charismatic migratory bird species.

273

274 **Funding**

275 This work was supported by the California Conservation Genomics Project, with funding provided
276 to the University of California by the State of California, State Budget Act of 2019 [UC Award ID
277 RSI-19-690224]. WLET was supported by the University of California, Los Angeles, Department
278 of Ecology and Evolutionary Biology, Lida Scott Brown Fellowship; and the National Science
279 Foundation, Graduate Research Fellowship [DGE-2034835]. Any opinions, findings, and
280 conclusions or recommendations expressed in this material are those of the authors and do not
281 necessarily reflect the views of the National Science Foundation.

282

283 **Acknowledgements**

284 PacBio Sequel II library prep and sequencing was carried out at the DNA Technologies and
285 Expression Analysis Cores at the UC Davis Genome Center, supported by NIH Shared
286 Instrumentation Grant 1S10OD010786-01. Deep sequencing of Omni-C libraries used the
287 Novaseq S4 sequencing platforms at the Vincent J. Coates Genomics Sequencing Laboratory at
288 UC Berkeley, supported by NIH S10 OD018174 Instrumentation Grant. We thank the staff at the
289 UC Davis DNA Technologies and Expression Analysis Cores and the UC Santa Cruz
290 Paleogenomics Laboratory for their diligence and dedication to generating high quality sequence

291 data. We thank Maeve Secor for help with fieldwork; Tara Luckau, Dr. Courtney Miller, and Dr.
292 Erin Toffelmier for help with coordination and sample submission.

293

294 **Data Availability**

295 Data generated for this study are available under NCBI BioProject PRJNA777222. Raw
296 sequencing data for individual with voucher LACM:122168 (NCBI BioSamples SAMN29044059,
297 SAMN29044060) are deposited in the NCBI Short Read Archive (SRA) under SRX16742538 for
298 PacBio HiFi sequencing data, and SRX16742539 and SRX16742540 for the Omni-C Illumina
299 sequencing data. GenBank accessions for both primary and alternate assemblies are
300 GCA_024362935.1 and GCA_024372515.1; and for genome sequences JANCRA000000000 and
301 JANCRB000000000. The GenBank organelle genome assembly for the mitochondrial genome is
302 CM044545.1. Assembly scripts and other data for the analyses presented can be found at the
303 following GitHub repository: www.github.com/ccgproject/ccgp_assembly

304

305 **References**

306 Abdennur, N., & Mirny, L. A. (2020). Cooler: Scalable storage for Hi-C data and other
307 genomically labeled arrays. *Bioinformatics*, 36(1), 311–316.
308 <https://doi.org/10.1093/bioinformatics/btz540>

309 Aguillon, S. M., Walsh, J., & Lovette, I. J. (2021). Extensive hybridization reveals multiple
310 coloration genes underlying a complex plumage phenotype. *Proceedings of the Royal
311 Society B: Biological Sciences*, 288(1943), 20201805.
312 <https://doi.org/10.1098/rspb.2020.1805>

313 Allio, R., Schomaker-Bastos, A., Romiguier, J., Prosdocimi, F., Nabholz, B., & Delsuc, F.

314 (2020). MitoFinder: Efficient automated large-scale extraction of mitogenomic data in

315 target enrichment phylogenomics. *Molecular Ecology Resources*, 20(4), 892–905.

316 <https://doi.org/10.1111/1755-0998.13160>

317 Bay, R. A., Harrigan, R. J., Underwood, V. L., Gibbs, H. L., Smith, T. B., & Ruegg, K. (2018).

318 Genomic signals of selection predict climate-driven population declines in a migratory

319 bird. *Science*, 359(6371), 83–86. <https://doi.org/10.1126/science.aan4380>

320 Browning, M. R. (1994). A taxonomic review of *Dendroica petechia* (Yellow Warbler) (Aves:

321 Parulinae). *PROCEEDINGS OF THE BIOLOGICAL SOCIETY OF WASHINGTON*,

322 107(1), 27–51.

323 Caballero-López, V., Lundberg, M., Sokolovskis, K., & Bensch, S. (2022). Transposable

324 elements mark a repeat-rich region associated with migratory phenotypes of willow

325 warblers (*Phylloscopus trochilus*). *Molecular Ecology*, 31(4), 1128–1141.

326 <https://doi.org/10.1111/mec.16292>

327 Camacho, C., Coulouris, G., Avagyan, V., Ma, N., Papadopoulos, J., Bealer, K., & Madden, T.

328 L. (2009). BLAST+: Architecture and applications. *BMC Bioinformatics*, 10(1), 421.

329 <https://doi.org/10.1186/1471-2105-10-421>

330 Challis, R., Richards, E., Rajan, J., Cochrane, G., & Blaxter, M. (2020). BlobToolKit –

331 Interactive Quality Assessment of Genome Assemblies. *G3 Genes|Genomes|Genetics*,

332 10(4), 1361–1374. <https://doi.org/10.1534/g3.119.400908>

333 Chavarria-Pizarro, T., Gomez, J. P., Ungvari-Martin, J., Bay, R., Miyamoto, M. M., & Kimball,

334 R. (2019). Strong phenotypic divergence in spite of low genetic structure in the endemic

335 Mangrove Warbler subspecies (*Setophaga petechia xanthotera*) of Costa Rica. *Ecology*
336 and *Evolution*, n/a(n/a). <https://doi.org/10.1002/ece3.5826>

337 Chaves, J. A., Parker, P. G., & Smith, T. B. (2012). Origin and population history of a recent
338 colonizer, the yellow warbler in Galápagos and Cocos Islands. *Journal of Evolutionary*
339 *Biology*, 25(3), 509–521. <https://doi.org/10.1111/j.1420-9101.2011.02447.x>

340 Chen, Y., Jiang, Z., Fan, P., Ericson, P. G. P., Song, G., Luo, X., Lei, F., & Qu, Y. (2022). The
341 combination of genomic offset and niche modelling provides insights into climate
342 change-driven vulnerability. *Nature Communications*, 13(1), Article 1.
343 <https://doi.org/10.1038/s41467-022-32546-z>

344 Cheng, H., Jarvis, E. D., Fedrigo, O., Koepfli, K.-P., Urban, L., Gemmell, N. J., & Li, H. (2022).
345 Haplotype-resolved assembly of diploid genomes without parental data. *Nature*
346 *Biotechnology*, 40(9), 1332–1335. <https://doi.org/10.1038/s41587-022-01261-x>

347 Collinge, S. K., Holyoak, M., Barr, C. B., & Marty, J. T. (2001). Riparian habitat fragmentation
348 and population persistence of the threatened valley elderberry longhorn beetle in central
349 California. *Biological Conservation*, 100(1), 103–113. [https://doi.org/10.1016/S0006-3207\(00\)00211-1](https://doi.org/10.1016/S0006-3207(00)00211-1)

351 Dahl, T. E. (1990). *Wetlands losses in the United States, 1780's to 1980's. Report to the*
352 *Congress* (PB-91-169284/XAB). National Wetlands Inventory, St. Petersburg, FL
353 (USA). <https://www.osti.gov/biblio/5527872-wetlands-losses-united-states-report-congress>

355 Davidson, C., Bradley Shaffer, H., & Jennings, M. R. (2001). Declines of the California Red-
356 Legged Frog: Climate, Uv-B, Habitat, and Pesticides Hypotheses. *Ecological*

357 *Applications*, 11(2), 464–479. [https://doi.org/10.1890/1051-0761\(2001\)011\[0464:DOTCRL\]2.0.CO;2](https://doi.org/10.1890/1051-0761(2001)011[0464:DOTCRL]2.0.CO;2)

359 Degrandi, T. M., Barcellos, S. A., Costa, A. L., Garnero, A. D. V., Hass, I., & Gunski, R. J.

360 (2020). Introducing the Bird Chromosome Database: An Overview of Cytogenetic

361 Studies in Birds. *Cytogenetic and Genome Research*, 160(4), 199–205.

362 <https://doi.org/10.1159/000507768>

363 Delmore, K., Illera, J. C., Pérez-Tris, J., Segelbacher, G., Lugo Ramos, J. S., Durieux, G.,

364 Ishigohoka, J., & Liedvogel, M. (2020). The evolutionary history and genomics of

365 European blackcap migration. *eLife*, 9, e54462. <https://doi.org/10.7554/eLife.54462>

366 DeSaix, M. G., George, T. L., Seglund, A. E., Spellman, G. M., Zavaleta, E. S., & Ruegg, K. C.

367 (2022). Forecasting climate change response in an alpine specialist songbird reveals the

368 importance of considering novel climate. *Diversity and Distributions*, 28(10), 2239–

369 2254. <https://doi.org/10.1111/ddi.13628>

370 Feng, S., Stiller, J., Deng, Y., Armstrong, J., Fang, Q., Reeve, A. H., Xie, D., Chen, G., Guo, C.,

371 Faircloth, B. C., Petersen, B., Wang, Z., Zhou, Q., Diekhans, M., Chen, W., Andreu-

372 Sánchez, S., Margaryan, A., Howard, J. T., Parent, C., ... Zhang, G. (2020). Dense

373 sampling of bird diversity increases power of comparative genomics. *Nature*, 587(7833),

374 Article 7833. <https://doi.org/10.1038/s41586-020-2873-9>

375 Fink, D., Auer, T., Johnston, A., Strimas-Mackey, M., Ligocki, S., Robinson, O., Hochachka,

376 W., Jaromczyk, L., Rodewald, A., Wood, C., Davies, I., & Spencer, A. (2022). *eBird*

377 *Status and Trends, Data Version: 2021; Released: 2022. Cornell Lab of Ornithology*,

378 Ithaca, New York. <https://doi.org/10.2173/ebirdst.2021>

379 Fitzpatrick, M. C., & Keller, S. R. (2015). Ecological genomics meets community-level
380 modelling of biodiversity: Mapping the genomic landscape of current and future
381 environmental adaptation. *Ecology Letters*, 18(1), 1–16.
382 <https://doi.org/10.1111/ele.12376>

383 Forester, B. R., Lasky, J. R., Wagner, H. H., & Urban, D. L. (2018). Comparing methods for
384 detecting multilocus adaptation with multivariate genotype–environment associations.
385 *Molecular Ecology*, 27(9), 2215–2233. <https://doi.org/10.1111/mec.14584>

386 Franchini, P., Irisarri, I., Fudickar, A., Schmidt, A., Meyer, A., Wikelski, M., & Partecke, J.
387 (2017). Animal tracking meets migration genomics: Transcriptomic analysis of a partially
388 migratory bird species. *Molecular Ecology*, 26(12), 3204–3216.
389 <https://doi.org/10.1111/mec.14108>

390 Ghurye, J., Pop, M., Koren, S., Bickhart, D., & Chin, C.-S. (2017). Scaffolding of long read
391 assemblies using long range contact information. *BMC Genomics*, 18(1), 527.
392 <https://doi.org/10.1186/s12864-017-3879-z>

393 Ghurye, J., Rhie, A., Walenz, B. P., Schmitt, A., Selvaraj, S., Pop, M., Phillippy, A. M., &
394 Koren, S. (2019). Integrating Hi-C links with assembly graphs for chromosome-scale
395 assembly. *PLOS Computational Biology*, 15(8), e1007273.
396 <https://doi.org/10.1371/journal.pcbi.1007273>

397 Gibbs, H. L., Dawson, R. J. G., & Hobson, K. A. (2000). Limited differentiation in microsatellite
398 DNA variation among northern populations of the yellow warbler: Evidence for male-
399 biased gene flow? *Molecular Ecology*, 9(12), 2137–2147. [https://doi.org/10.1046/j.1365-294X.2000.01136.x](https://doi.org/10.1046/j.1365-
400 294X.2000.01136.x)

401 Goloborodko, A., Abdennur, N., Venev, S., hbbrandao, & gfudenberg. (2018).
402 *mirnylab/pairtools: V0.2.0* [Computer software]. Zenodo.
403 <https://doi.org/10.5281/zenodo.1490831>
404 Gopalakrishnan, S., Samaniego Castruita, J. A., Sinding, M.-H. S., Kuderna, L. F. K.,
405 Räikkönen, J., Petersen, B., Sicheritz-Ponten, T., Larson, G., Orlando, L., Marques-
406 Bonet, T., Hansen, A. J., Dalén, L., & Gilbert, M. T. P. (2017). The wolf reference
407 genome sequence (*Canis lupus lupus*) and its implications for *Canis* spp. Population
408 genomics. *BMC Genomics*, 18(1), 495. <https://doi.org/10.1186/s12864-017-3883-3>
409 Gurevich, A., Saveliev, V., Vyahhi, N., & Tesler, G. (2013). QUAST: Quality assessment tool
410 for genome assemblies. *Bioinformatics*, 29(8), 1072–1075.
411 <https://doi.org/10.1093/bioinformatics/btt086>
412 Heath, S. K., & Ballard, G. (2003). *Patterns of Breeding Songbird Diversity and Occurrence in*
413 *Riparian Habitats of the Eastern Sierra Nevada*.
414 Hobart, H. H. (1991). *Comparative karyology in nine-primaried oscines (Aves)*.
415 <https://repository.arizona.edu/handle/10150/185492>
416 Jarvis, E. D. (2016). Perspectives from the Avian Phylogenomics Project: Questions that Can Be
417 Answered with Sequencing All Genomes of a Vertebrate Class. *Annual Review of Animal*
418 *Biosciences*, 4(1), 45–59. <https://doi.org/10.1146/annurev-animal-021815-111216>
419 Kapusta, A., & Suh, A. (2017). Evolution of bird genomes—A transposon’s-eye view. *Annals of*
420 *the New York Academy of Sciences*, 1389(1), 164–185.
421 <https://doi.org/10.1111/nyas.13295>
422 Kerpedjiev, P., Abdennur, N., Lekschas, F., McCallum, C., Dinkla, K., Strobelt, H., Luber, J. M.,
423 Ouellette, S. B., Azhir, A., Kumar, N., Hwang, J., Lee, S., Alver, B. H., Pfister, H.,

424 Mirny, L. A., Park, P. J., & Gehlenborg, N. (2018). HiGlass: Web-based visual
425 exploration and analysis of genome interaction maps. *Genome Biology*, 19(1), 125.
426 <https://doi.org/10.1186/s13059-018-1486-1>

427 Klein, N. K., & Brown, W. M. (1994). Intraspecific Molecular Phylogeny in the Yellow Warbler
428 (Dendroica petechia), and Implications for Avian Biogeography in the West Indies.
429 *Evolution*, 48(6), 1914. <https://doi.org/10.2307/2410517>

430 Korlach, J., Gedman, G., Kingan, S. B., Chin, C.-S., Howard, J. T., Audet, J.-N., Cantin, L., &
431 Jarvis, E. D. (2017). De novo PacBio long-read and phased avian genome assemblies
432 correct and add to reference genes generated with intermediate and short reads.
433 *GigaScience*, 6(10), gix085. <https://doi.org/10.1093/gigascience/gix085>

434 Krueper, D. J. (1996). Effects of livestock management on Southwestern riparian ecosystems. In:
435 *Shaw, Douglas W.; Finch, Deborah M., Tech Coords. Desired Future Conditions for*
436 *Southwestern Riparian Ecosystems: Bringing Interests and Concerns Together. 1995*
437 *Sept. 18-22, 1995; Albuquerque, NM. General Technical Report RM-GTR-272. Fort*
438 *Collins, CO: U.S. Department of Agriculture, Forest Service, Rocky Mountain Forest and*
439 *Range Experiment Station. p. 281-301.*, 272, 281–301.

440 Lamichhaney, S., Han, F., Berglund, J., Wang, C., Almén, M. S., Webster, M. T., Grant, B. R.,
441 Grant, P. R., & Andersson, L. (2016). A beak size locus in Darwin's finches facilitated
442 character displacement during a drought. *Science*, 352(6284), 470–474.
443 <https://doi.org/10.1126/science.aad8786>

444 Li, H. (2013). Aligning sequence reads, clone sequences and assembly contigs with BWA-MEM
445 (arXiv:1303.3997). arXiv. <https://doi.org/10.48550/arXiv.1303.3997>

446 Machkour-M'Rabet, S., Santamaría-Rivero, W., Dzib-Chay, A., Cristiani, L. T., & MacKinnon-

447 Haskins, B. (2023). Multi-character approach reveals a new mangrove population of the

448 Yellow Warbler complex, *Setophaga petechia*, on Cozumel Island, Mexico. *PLOS ONE*,

449 18(6), e0287425. <https://doi.org/10.1371/journal.pone.0287425>

450 Manni, M., Berkeley, M. R., Seppey, M., Simão, F. A., & Zdobnov, E. M. (2021). BUSCO

451 Update: Novel and Streamlined Workflows along with Broader and Deeper Phylogenetic

452 Coverage for Scoring of Eukaryotic, Prokaryotic, and Viral Genomes. *Molecular Biology*

453 and Evolution

454 and Evolution

455 38(10), 4647–4654. <https://doi.org/10.1093/molbev/msab199>

456 Mérot, C., Oomen, R. A., Tigano, A., & Wellenreuther, M. (2020). A Roadmap for

457 Understanding the Evolutionary Significance of Structural Genomic Variation. *Trends in*

458 *Ecology & Evolution*, 35(7), 561–572. <https://doi.org/10.1016/j.tree.2020.03.002>

459 Milot, E., Gibbs, H. L., & Hobson, K. A. (2000). Phylogeography and genetic structure of

460 northern populations of the yellow warbler (*Dendroica petechia*). *Molecular Ecology*,

461 9(6), 667–681. <https://doi.org/10.1046/j.1365-294x.2000.00897.x>

462 Peona, V., Blom, M. P. K., Xu, L., Burri, R., Sullivan, S., Bunikis, I., Liachko, I., Haryoko, T.,

463 Jönsson, K. A., Zhou, Q., Irestedt, M., & Suh, A. (2021). Identifying the causes and

464 consequences of assembly gaps using a multiplatform genome assembly of a bird-of-

465 paradise. *Molecular Ecology Resources*, 21(1), 263–286. <https://doi.org/10.1111/1755-0998.13252>

466 Phillips, S. E., Hamilton, L. P., & Kelly, P. A. (2005). *Assessment of habitat conditions for the*

467 *Riparian Brush Rabbit on the San Joaquin River National Wildlife Refuge, California*.

468 Poff, B., Koestner, K. A., Neary, D. G., & Merritt, D. (2012). *Threats to western United States*

469 *riparian ecosystems: A bibliography* (RMRS-GTR-269). U.S. Department of Agriculture,

469 Forest Service, Rocky Mountain Research Station. <https://doi.org/10.2737/RMRS-GTR-269>

470

471 Prasad, A., Lorenzen, E. D., & Westbury, M. V. (2022). Evaluating the role of reference-genome

472 phylogenetic distance on evolutionary inference. *Molecular Ecology Resources*, 22(1),

473 45–55. <https://doi.org/10.1111/1755-0998.13457>

474 Ramírez, F., Bhardwaj, V., Arrigoni, L., Lam, K. C., Grüning, B. A., Villaveces, J., Habermann,

475 B., Akhtar, A., & Manke, T. (2018). High-resolution TADs reveal DNA sequences

476 underlying genome organization in flies. *Nature Communications*, 9(1), Article 1.

477 <https://doi.org/10.1038/s41467-017-02525-w>

478 Ranallo-Benavidez, T. R., Jaron, K. S., & Schatz, M. C. (2020). GenomeScope 2.0 and

479 Smudgeplot for reference-free profiling of polyploid genomes. *Nature Communications*,

480 11(1), Article 1. <https://doi.org/10.1038/s41467-020-14998-3>

481 Rhie, A., McCarthy, S. A., Fedrigo, O., Damas, J., Formenti, G., Koren, S., Uliano-Silva, M.,

482 Chow, W., Fungtammasan, A., Gedman, G. L., Cantin, L. J., Thibaud-Nissen, F.,

483 Haggerty, L., Lee, C., Ko, B. J., Kim, J., Bista, I., Smith, M., Haase, B., ... Jarvis, E. D.

484 (2020). Towards complete and error-free genome assemblies of all vertebrate species.

485 *bioRxiv*, 2020.05.22.110833. <https://doi.org/10.1101/2020.05.22.110833>

486 Rhie, A., McCarthy, S. A., Fedrigo, O., Damas, J., Formenti, G., Koren, S., Uliano-Silva, M.,

487 Chow, W., Fungtammasan, A., Kim, J., Lee, C., Ko, B. J., Chaisson, M., Gedman, G. L.,

488 Cantin, L. J., Thibaud-Nissen, F., Haggerty, L., Bista, I., Smith, M., ... Jarvis, E. D.

489 (2021). Towards complete and error-free genome assemblies of all vertebrate species.

490 *Nature*, 592(7856), Article 7856. <https://doi.org/10.1038/s41586-021-03451-0>

491 Salgado-Ortiz, J., Marra, P. P., Sillett, T. S., & Robertson, R. J. (2008). Breeding Ecology of the
492 Mangrove Warbler (*Dendroica Petechia Bryanti*) and Comparative Life History of the
493 Yellow Warbler Subspecies ComplexEcología Reproductiva de *Dendroica petechia*
494 bryanti y Comparación de los Rasgos de Historia de Vida de las Subespecies del
495 Complejo de *Dendroica petechia*Salgado-Ortiz et al.Breeding Ecology of the Mangrove
496 Warbler. *The Auk*, 125(2), 402–410. <https://doi.org/10.1525/auk.2008.07012>

497 Sauer, J. R., Hines, J. E., Fallon, J. E., & Pardiek, K. L. (2014). *The North American Breeding*
498 *Bird Survey* (Version 02.19) [dataset]. U.S. Geological Survey Patuxent Wildlife
499 Research Center.

500 Shaffer, H. B., Toffelmier, E., Corbett-Detig, R. B., Escalona, M., Erickson, B., Fiedler, P.,
501 Gold, M., Harrigan, R. J., Hodges, S., Luckau, T. K., Miller, C., Oliveira, D. R., Shaffer,
502 K. E., Shapiro, B., Sork, V. L., & Wang, I. J. (2022). Landscape Genomics to Enable
503 Conservation Actions: The California Conservation Genomics Project. *Journal of*
504 *Heredity*, esac020. <https://doi.org/10.1093/jhered/esac020>

505 Shuford, W. D., Gardali, T., Western Field Ornithologists, California, & Department of Fish and
506 Game. (2008). *California bird species of special concern: A ranked assessment of*
507 *species, subspecies, and distinct populations of birds of immediate conservation concern*
508 *in California*. Western Field Ornithologists ; California Dept. of Fish and Game.
509 <http://books.google.com/books?id=9INFAQAAIAAJ>

510 Sim, S. B., Corpuz, R. L., Simmonds, T. J., & Geib, S. M. (2022). HiFiAdapterFilt, a memory
511 efficient read processing pipeline, prevents occurrence of adapter sequence in PacBio
512 HiFi reads and their negative impacts on genome assembly. *BMC Genomics*, 23(1), 157.
513 <https://doi.org/10.1186/s12864-022-08375-1>

514 Toews, D. P. L., Taylor, S. A., Vallender, R., Brelsford, A., Butcher, B. G., Messer, P. W., &
515 Lovette, I. J. (2016). Plumage Genes and Little Else Distinguish the Genomes of
516 Hybridizing Warblers. *Current Biology*, 26(17), 2313–2318.
517 <https://doi.org/10.1016/j.cub.2016.06.034>

518 Uliano-Silva, M., Nunes, J. G. F., Krasheninnikova, K., & McCarthy, S. A. (2021).
519 *marcelauliano/MitoHiFi: MitoHifi_v2.0* [Computer software]. Zenodo.
520 <https://doi.org/10.5281/zenodo.5205678>

521 Wellenreuther, M., & Bernatchez, L. (2018). Eco-Evolutionary Genomics of Chromosomal
522 Inversions. *Trends in Ecology & Evolution*, 33(6), 427–440.
523 <https://doi.org/10.1016/j.tree.2018.04.002>

524 Wilson, C. M., & Holberton, R. L. (2004). Individual Risk Versus Immediate Reproductive
525 Success: A Basis for Latitudinal Differences in the Adrenocortical Response to Stress in
526 Yellow Warblers (*Dendroica Petechia*). *The Auk*, 121(4), 1238–1249.
527 <https://doi.org/10.1093/auk/121.4.1238>

528

529 **Supplementary Material**

530 **Figure S1.** Visual overview of genome assembly metrics for alternate assembly (bSetPet1.0.a).

531 **Tables**

532 **Table 1.** Assembly pipeline and software used for assembly of the Yellow Warbler genome.

533 Software citations are listed in the text.

Purpose	Software ^a	Version
Assembly		
adapters	HiFiAdapterFilt	Commit 64d1c7b
K-mer counting	Meryl (k=21)	1
Estimation of genome size and heterozygosity	GenomeScope	2
<i>De novo assembly (contiging)</i>	HiFiasm (Hi-C Mode, --primary, output p_ctg.hap1, p_ctg.hap2)	0.16.1-r375
Scaffolding		
Omni-C data alignment	Arima Genomics Mapping Pipeline	Commit 2e74ea4
Omni-C Scaffolding	SALSA (-DNASE, -i 20, -p yes)	2
Gap closing	YAGCloser (-mins 2 -f 20 -mcc 2 -prt 0.25 -eft 0.2 -pld 0.2)	Commit 0e34c3b
Omni-C Contact map generation		
Short-read alignment	BWA-MEM (-5SP)	0.7.17-r1188
SAM/BAM processing	samtools	1.11
SAM/BAM filtering	pairtools	0.3.0
Pairs indexing	pairix	0.3.7
Matrix generation	cooler	0.8.10
Matrix balancing	hicExplorer (hicCorrectmatrix correct --filterThreshold -2 4)	3.6
Contact map visualization	HiGlass	2.1.11
	PretextMap	0.1.4
	PretextView	0.1.5
	PretextSnapshot	0.0.3
Genome quality assessment		
Basic assembly metrics	QUAST (--est-ref-size)	5.0.2
Assembly completeness	BUSCO (-m geno, -l aves)	5.0.0
	Merqury	2020-01-29
Contamination screening		
Local alignment tool	BLAST+ (-db nt, -outfmt '6 qseqid staxids bitscore std', -max_target_seqs 1, -max_hsps 1, -evalue 1e-25)	2.1
General contamination screening	BlobToolKit (PacBio HiFi Coverage, NCBI Taxa ID = 123631, BUSCODOB = aves)	2.3.3

534

^aOptions detailed for non-default parameters.

535 **Table 2.** Sequencing and assembly statistics and accession information for the primary and
 536 alternate assemblies of the Yellow Warbler (*Setophaga petechia*) genome.

Bio Projects & Vouchers	CCGP NCBI BioProject Genera NCBI BioProject Species NCBI BioProject NCBI BioSample Specimen identification		PRJNA720569 PRJNA765861 PRJNA777222 SAMN29044059, SAMN29044060 LACM:Birds122168		
	NCBI Genome accessions	Primary	Alternate		
	Assembly accession	JANCRA000000000	JANCRB000000000		
	Genome sequences	GCA_024362935.1	GCA_024372515.1		
Genome Sequence	PacBio HiFi reads Omni-C Illumina reads	Run Accession Run Accession	1 PACBIO_SMRT (Sequel II) run: 2.7M spots, 46.9G bases, 35.6Gb downloads SRX16742538 1 ILLUMINA (Illumina NovaSeq 6000) run: 85.3M spots, 25.8G bases, 8.6Gb SRX16742539, SRX16742540		
Genome Assembly Quality Metrics	Assembly identifier (Quality code ^a) HiFi Read coverage ^b		bSetPet1(6.7.P6.Q62.C) 40.87X		
	Number of contigs Contig N50 (bp) Contig NG50 ^b Longest Contigs Number of scaffolds Scaffold N50 Scaffold NG50 ^b Largest scaffold Size of final assembly Phased block NG50 ^b Gaps per Gbp (# Gaps) Indel QV (Frame shift) Base pair QV	Primary	Alternate		
	971 6,807,045 7,219,428 53,526,829 687 21,188,473 21,769,140 66,288,485 1,222,385,128 7,391,252 232(284) 41.54557 62.3497	971 6,807,045 7,219,428 53,526,829 687 21,188,473 20,409,353 74,562,066 1,249,765,916 9,325,426 197(246) 40.4344848 62.7988	776 8,368,636 8,924,963 40,027,624 530 21,188,473 20,409,353 74,562,066 1,249,765,916 9,325,426 197(246) 40.4344848 62.7988		
	k-mer completeness	84.9555	81.57 Full assembly = 99.2811		
BUSCO completeness (aves) n=	C^c P^d A^d	S^c 96.00% 93.50%	D^c 0.70% 1.00%	F^c 0.60% 0.60%	M^c 3.40% 5.90%
Organelles		1 complete mitochondrial sequence		CM044545.1	

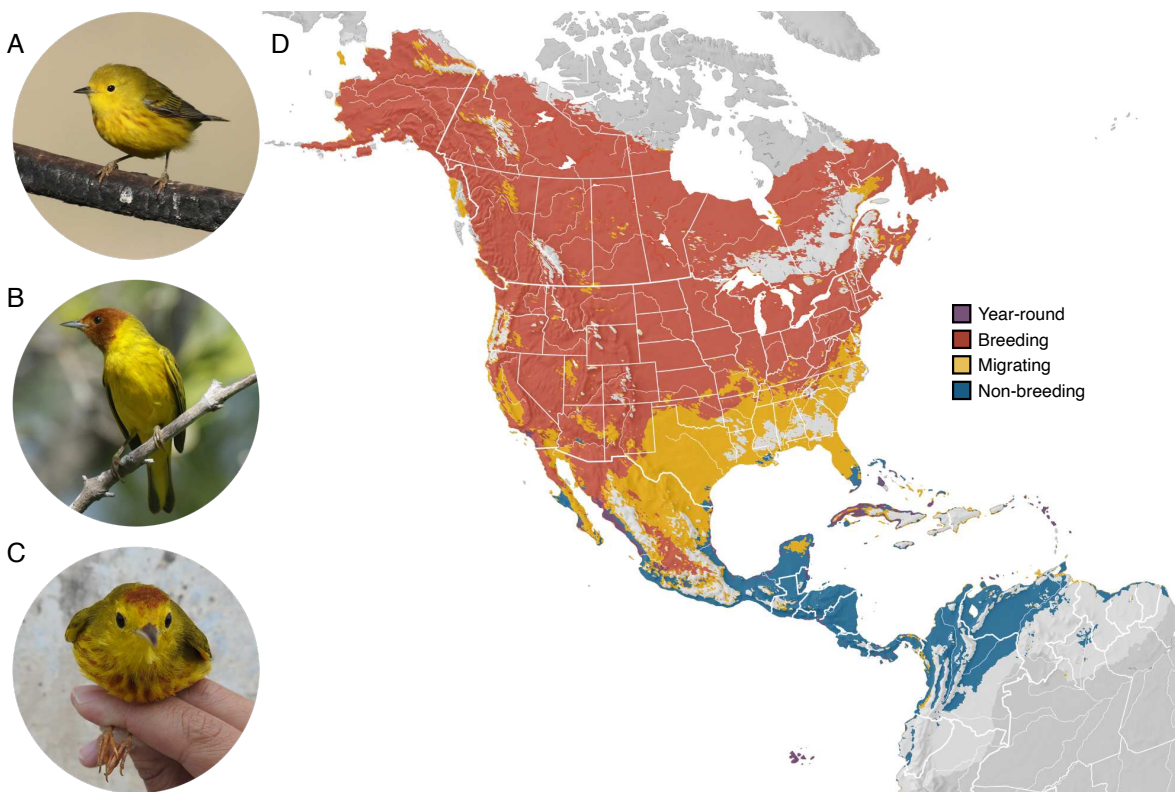
^aAssembly quality code x.y.P.Q.C derived notation, from (Rhie et al. 2021). x = log10[contig NG50]; y = log10[scaffold NG50]; P = log10 [phased block NG50]; Q = Phred base accuracy QV (Quality value); C = % genome represented by the first 'n' scaffolds, following a known karyotype for *S. petechia* of 2n=80 (Bird Chromosome Database, Chromosome number data V3.0/2022; Degrandi et al., 2020; Hobart, 1991). Quality code for all the assembly denoted by primary assembly (bSetPet1.0.p)

^bRead coverage and NGx statistics have been calculated based on the estimated genome size of 1.14 Gb

^cBUSCO Scores. Complete BUSCOs (C). Complete and single-copy BUSCOs (S). Complete and duplicated BUSCOs (D). Fragmented BUSCOs (F). Missing BUSCOs (M).

^d(P)primary and (A)lternate assembly values.

538 **Figures**

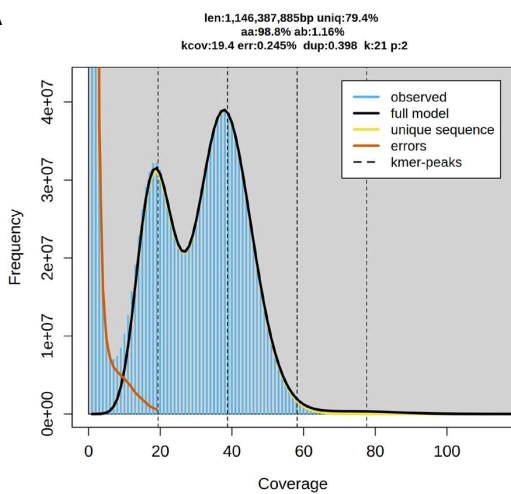


539

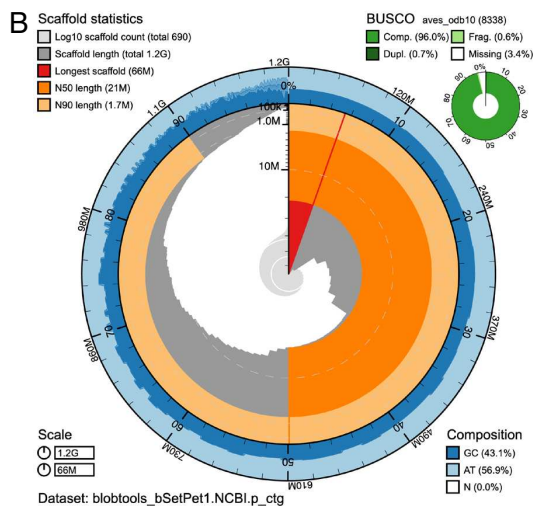
540 **Figure 1.** Geographic variation and distribution of Yellow Warblers (*Setophaga petechia*). A) The
541 Northern (*aestiva*) group includes migratory subspecies with chestnut streaking on the breast.
542 Northern subspecies breed in North America and winter in Central and northern South America.
543 Photo taken by R. S. Terrill at Piute Ponds, Los Angeles, CA, USA. B) The Mangrove
544 (*erithachorides*) group includes resident subspecies with a characteristic all chestnut head.
545 Mangrove subspecies inhabit mangroves along the coasts of Central and northern South America
546 year-round. Photo taken by R. S. Terrill on Isla Holbox, Quintana Roo, MX. C) The Galapagos
547 (*aureola*) and Golden (*petechia*) subspecies groups includes resident subspecies with a chestnut
548 cap and thick breast streaking except for *S. p. ruficapilla* from Martinique which exhibits the
549 Mangrove phenotype. Populations of the Galapagos subspecies are found on the Galapagos Islands

550 and Cocos Island off Costa Rica and Golden subspecies are found on the islands of the Caribbean.
551 Photo taken by W. L. E. Tsai on Isla Cozumel, Quintana Roo, MX. D) Map of species
552 distributional abundance (Fink et al., 2022). Shaded colors indicate seasonal shifts in distributions:
553 year-round (purple), breeding (red), migrating (yellow), and non-breeding (blue).

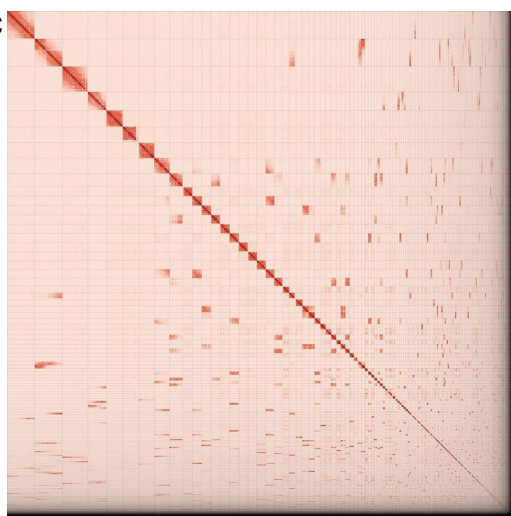
A



B



C



555 **Figure 2.** Visual overview of genome assembly metrics. A) Kmer spectra output generated from
556 PacBio HiFi data without adapters using GenomScope2.0. The bimodal pattern observed
557 corresponds to a diploid genome. K-mers covered at lower coverage and lower frequency
558 correspond to differences between haplotypes, whereas the higher coverage and higher frequency
559 k-mers correspond to the similarities between haplotypes. B) BlobToolKit Snail plot showing a
560 graphical representation of the quality metrics presented in Table 2 for the *Setophaga petechia*
561 primary assembly (bSetPet1.0.p). The plot circle represents the full size of the assembly. From the
562 inside-out, the central plot covers scaffold and length-related metrics. The central light gray spiral
563 shows the cumulative scaffold count with a white line at each order of magnitude. The red line
564 represents the size of the longest scaffold; all other scaffolds are arranged in size-order moving
565 clockwise around the plot and drawn in gray starting from the outside of the central plot. Dark and
566 light orange arcs show the scaffold N50 and scaffold N90 values. The outer light and dark blue
567 ring show the mean, maximum, and minimum GC versus AT content at 0.1% intervals (Challis et
568 al. 2020). C) Omni-C contact map for the primary genome assembly generated with
569 PretextSnapshot. Omni-C contact maps translate proximity of genomic regions in 3D space to
570 contiguous linear organization. Each cell in the contact map corresponds to sequencing data
571 supporting the linkage (or join) between 2 such regions. Scaffolds are separated by black lines and
572 higher density corresponds to higher levels of fragmentation.

573

574

575

576

577

578